

SHE: A Fast and Accurate Privacy-Preserving Deep Neural Network Via Leveled TFHE and Logarithmic Data Representation

Qian Lou

Indiana University Bloomington

louqian@iu.edu

Lei Jiang

Indiana University Bloomington

jiang60@iu.edu

Abstract

Homomorphic Encryption (HE) is one of the most promising security solutions to emerging Machine Learning as a Service (MLaaS). Several Leveled-HE (LHE)-enabled Convolutional Neural Networks (LHECNNs) are proposed to implement MLaaS to avoid the large bootstrapping overhead. However, prior LHECNNs have to pay significant computational overhead but achieve only low inference accuracy, due to their polynomial approximation activations and poolings. Stacking many polynomial approximation activation layers in a network greatly reduces the inference accuracy, since the polynomial approximation activation errors lead to a low distortion of the output distribution of the next batch normalization layer. So the polynomial approximation activations and poolings have become the obstacle to a fast and accurate LHECNN model.

In this paper, we propose a Shift-accumulation-based LHE-enabled deep neural network (SHE) for fast and accurate inferences on encrypted data. We use the binary-operation-friendly leveled-TFHE (LTFHE) encryption scheme to implement ReLU activations and max poolings. We also adopt the logarithmic quantization to accelerate inferences by replacing expensive LTFHE multiplications with cheap LTFHE shifts. We propose a mixed bitwidth accumulator to expedite accumulations. Since the LTFHE ReLU activations, max poolings, shifts and accumulations have small multiplicative depth, SHE can implement much deeper network architectures with more convolutional and activation layers. Our experimental results show SHE achieves the state-of-the-art inference accuracy and reduces the inference latency by 76.21% ~ 94.23% over prior LHECNNs on MNIST and CIFAR-10.

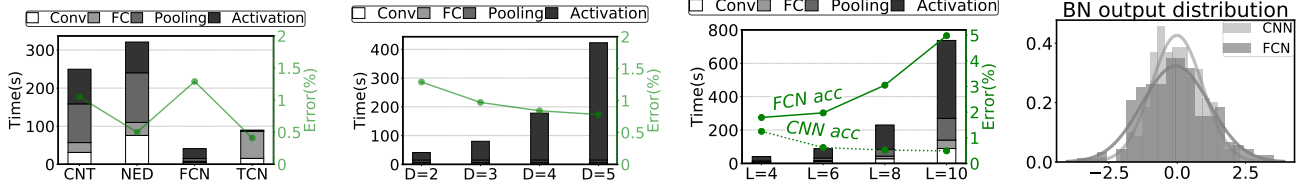
1. Introduction

Machine Learning as a Service (MLaaS) is an effective method for clients to run their computationally expensive Convolutional Neural Network (CNN) inferences [1] on

powerful cloud servers. CNN inferences have to access to client raw data, which potentially introduces security and privacy risks. So there is a strong and urgent need to ensure the confidentiality of healthcare records, financial data and other sensitive information of clients uploaded to cloud servers. Recent works [2, 3, 4, 1, 5] employ leveled Homomorphic Encryption (LHE) to perform CNN inferences over encrypted data. During the LHE-enabled MLaaS, a client encrypts the sensitive data and sends it to a server. Since only the client has the private key, the server cannot decrypt the input nor the output. The server produces an encrypted inference output and returns it to the client. The client privacy is preserved in this pipeline for both inputs and outputs.

However, prior LHE-enabled CNNs (LHECNNs) [2, 3, 4, 1, 5] suffer from low inference accuracy and long inference latency. TAPAS [5] and DiNN [1] adopt only 1-bit CNN weights, inputs and *sign* activations, so they degrade 3%~6.2% inference accuracy even on tiny hand-written digit dataset MNIST [6]. Since HE supports only polynomial computations, CryptoNet (CNT) [2], NED [3] and Faster Cryptonet (FCN) [4] have to use the *square* activations instead of *ReLU*, and thus fail to obtain the state-of-the-art inference accuracy. For instance, FCN achieves only 76.72% inference accuracy on CIFAR-10 dataset [7], while the accuracy of an unencrypted CNN model with *ReLU* activations is 93.72%. Although it is possible to improve the encrypted inference accuracy by enlarging the degree of the polynomial approximation activations (PAAs), the PAA computational overhead increases exponentially with its degree. With even a degree-2 *square* activation, prior LHECNNs, e.g., CNT and NED, still require hundreds of seconds to perform an inference on an encrypted MNIST image.

Moreover, the PAA is not compatible with a deep network consisting of many convolutional and activation layers. Stacking many convolutional and PAA layers in a network actually decreases the inference accuracy [8], since the PAA approximation errors lead to a low distortion of the output distribution of the next batch normalization layer. As a result, no prior LHECNN fully supports deep networks computing



(a) Perf. and acc. of prior LHECNNs. (b) FCN PAAPs + various degrees (Ds). (c) FCN + various PAA layers (L) #s. (d) The output of the 9th BN layer.

Figure 1. The performance and accuracy bottlenecks of prior LHECNNs testing MNIST: the PAAP (Conv: convolutional layer; FC: fully-connected layer; Pooling: pooling layer; and Activation: batch normalization (BN) + activation layer).

the large ImageNet [9]. For instance, FCN [4] can compute only a part (i.e., 3 convolutional layers with *square* activations) of a CNN testing ImageNet on the server but leave the other parts of the CNN to the client.

2. Background and Motivation

Threat model. In the MLaaS paradigm, an inherent risk of data transmission exists when clients send sensitive input data or servers return sensitive output results back to clients. Although a strongly encryption scheme can be used to encrypt data sent to the cloud, untrusted servers [2, 3, 4] can make data leakage happen. HE is one of the most promising encryption techniques to enable a server to perform CNN inference over encrypted data. A client sends encrypted data to a server performing encrypted inference without decrypting the data or the client private key. Only the client can decrypt the inference result using the private key.

Homomorphic Encryption. An encryption scheme defines an encryption function $\epsilon()$ encoding data to ciphertexts (encrypted data), and a decryption function $\delta()$ mapping ciphertexts back to plaintexts (original data). In a public-key encryption, the ciphertexts x can be computed as $\epsilon(x, k_{pub})$, where k_{pub} is the public key. The decryption can be done through $\delta(\epsilon(x, k_{pub}), k_{sec}) = x$, where k_{sec} is the secret key. An encryption scheme is *homomorphic* in an operation \odot if there is another operation \oplus such that $\epsilon(x, k_{pub}) \oplus \epsilon(y, k_{pub}) = \epsilon(x \odot y, k_{pub})$. To prevent threats on untrusted servers, fully HE [10] enables an unlimited number of computations over ciphertexts. However, each computation introduces noise into the ciphertexts. After a certain number of computations, the noise grows too large so that the ciphertexts cannot be decrypted successfully. A *bootstrapping* [11] is required to keep the noise in check without decrypting. Unfortunately, the bootstrapping is extremely slow, due to its high computational complexity. Leveled HE (LHE) [12] is proposed to accelerate encrypted computations without bootstrapping. But LHE allows to compute polynomial functions of only a maximal degree on the ciphertexts. Before applying LHE, the complexity of the target arithmetic circuit processing the ciphertexts must be known in advance. Compared to Multiple Party Computation (MPC) [13, 14, 15, 16, 17, 18], LHE has much less communication overhead. When applying MPC in MLaaS,

DeepSecure [15] has to exchange 722GB data between the client and the server for only a 5-layer CNN inference on a tiny MNIST image.

TFHE. TFHE [19, 16] is a HE cryptosystem that expresses ciphertexts over the torus modulo 1. It supports both fully and leveled HE schemes. Like the other HE cryptosystems including BFV/BGV [20], FV-RNS [21] and HEAAN [22], TFHE is also based on the Ring-LWE, but it can perform very fast binary operations over encrypted binary bits. Therefore, unlike the other HE cryptosystems approximating the activation by expensive polynomial operations, TFHE can naturally implement *ReLU* activations and max poolings by Boolean operations. In this paper, we use TFHE for our design without its batching technology [19]. Although the ciphertext batching may greatly improve the LHECNN model inference throughput by packing multiple (e.g. 8K) datasets into a homomorphic operation, it has to select more numerous and restricted NTT points, force specific computations away from NTT, and add large computational cost [4]. Moreover, it is difficult for one client to batch 8K requests together sharing the same secret key. In fact, a client often needs to conduct inferences on only few images [23].

Motivation. As Figure 1 describes, prior LHECNNs suffer from low inference accuracy and long inference latency, because of the polynomial approximation activations (PAAs) and poolings. CryptoNet (CNT) [2] and Faster CryptoNet (FCN) [4] add a batch normalization layer before each activation layer. They also use *square* (polynomials with degree-2) activations and scaled mean poolings to replace *ReLU*s and max poolings, respectively. As Figure 1(a) shows, the *square* activation reduces the inference accuracy by 0.82% compared to unencrypted models on MNIST. Although increasing the degree of polynomials can improves their inference accuracy, the computing overhead of activation layers also exponentially increases as shown in Figure 1(b). NED [3] also uses high-degree PAAs to obtain nearly no accuracy loss, but its inference latency is much longer than CNT. For CNT, NED and FCN, the PAA layers occupies 65.7% ~ 81.2% of total inference time. Integrating more convolutional, activation and pooling layers in a network cannot improve the inference accuracy neither. As Figure 1(c) shows, an unencrypted CNN model (CNN) achieves higher inference accuracy with more layers, but

the inference accuracy of the LHE-enabled FCN decreases when having more convolutional and activation layers. This is because the *square* approximation errors result in a low distortion of the output distribution of the batch normalization layer. Figure 1(d) illustrates such an output distribution distortion of the 9th batch normalization layer in a 12-layer LHE-enabled FCN.

Name	Encry.	Sche.	ReLU	MaxPool	NoConv	DeepNet
CNT[2]	YASHE		\times	\times	\times	\times
NED[3]	BGV		\times	\times	\times	\times
FCN[4]	FV-RNS		\times	\times	\times	\times
DiNN[1]	TFHE		\times	\times	\checkmark	\times
TAPAS[5]	TFHE		\times	\times	\checkmark	\times
SHE	TFHE		\checkmark	\checkmark	\checkmark	\checkmark

Table 1. The comparison of LHECNNs.

Comparison against prior works. Table 1 compares our SHE against prior LHECNNs including CryptoNet (CNT) [2], NED [3], Faster CryptoNet (FCN) [4], DiNN [1] and TAPAS [5]. Due to the limitation of non-TFHE schemes, CNT, NED and FCN cannot support *ReLU* and max poolings. They are also slowed down by expensive homomorphic multiplications. Although DiNN [1] and TAPAS [5] binarize weights, inputs and activations to avoid homomorphic multiplications, their accuracy is low.

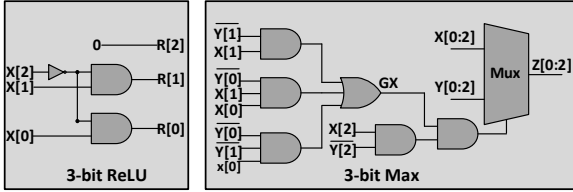


Figure 2. A 3-bit ReLU unit (X : input; R : output) and a 3-bit max pooling unit (X and Y : inputs; Z : output).

3. SHE

3.1. ReLU Activation and Max Pooling

The rectifier ($ReLU(x) = \max(x, 0)$) is one of the most widely adopted activation functions, while the max pooling is a sample-based discretization process heavily used in state-of-the-art CNN models. Prior BF/V- and FV-RNS-based LHECNNs [2, 4] approximate both $ReLU(x)$ and max pooling by linear polynomials leading to significant inference accuracy degradation and substantial computing overhead. Existing TFHE-based CNN models [1, 5] use the 1-bit *sign()* function to implement binarized activations that also introduce substantial accuracy loss.

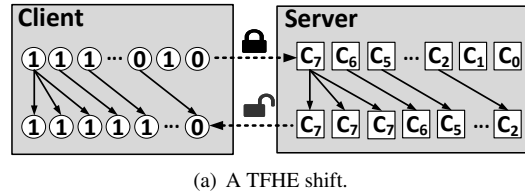
In this paper, we propose an accurate homomorphic *ReLU* function and a homomorphic max pooling operation. TFHE can implement any 2-input binary homomorphic operation, e.g., AND, OR, NOT, and MUX, over encrypted binary data by a deterministic automaton, a Boolean gate or a look-up table [19, 16]. In this way, as Figure 2 exhibits, we can connect the TFHE homomorphic Boolean gates to

construct a *ReLU* unit and a max pooling unit. A > 2 -input TFHE gate can be divided into multiple 2-input TFHE gates.

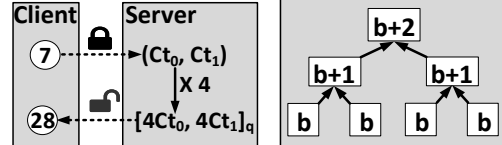
3.2. Logarithmic Quantization

When we implemented the Faster CryptoNet (FCN) through TFHE Boolean gates, as Figure 1(a) shows, we observe that the TFHE-based model (TFC) although has the same network architecture as FCN, its inference latency is much longer. This is because TFHE is not designed and optimized for matrix multiplications or other repetitive tasks. So the convolutional and fully-connected layers of TFC have become the new performance bottleneck.

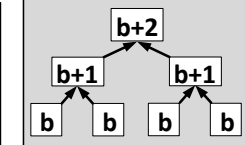
To reduce the matrix multiplication computing overhead, we logarithmically quantize the floating-point weights into their power-of-2 representations [24, 25], so that we can replace all multiplications in our CNN inference by shifts and accumulations. Prior works [26, 24, 25] suggest the logarithmic quantization even with weight pruning still achieves the same inference accuracy as full-precision models. In a logarithmically quantized CNN model $weight^T * input$ is approximately equivalent to $\sum_{i=1}^n input_i \times 2^{weightQ_i}$, and converted to $\sum_{i=1}^n binaryshift(input_i, weightQ_i)$, where $weightQ_i = Quantize(\log_2(weight_i))$, $Quantize(x)$ quantizes x to the closest integer and $binaryshift(a, b)$ shifts a by b bits in fixed-point arithmetic¹.



(a) A TFHE shift.



(b) A shift in others.



(c) A mixed-bitwidth acc.

Figure 3. Logarithmic quantization in various HE cryptosystems.

As Figure 3(a) highlights, the homomorphic shift operation of TFHE is cheap. TFHE encrypts the plaintext bit by bit. Moreover, it keeps the order of the ciphertext the same as that of the plaintext. A TFHE homomorphic arithmetic shift just copies the encrypted sign bit and the encrypted data to the shifted positions, so it only costs $\sim 100ns$ on a core of our CPU baseline. On the contrary, in other HE schemes, e.g., B/FV [20], FV-RNS [21] and HEAAN [22], a homomorphic arithmetic shift is equivalent to a homomorphic multiplication, as they encrypt each floating point number of plaintext as a whole shown in Figure 3(b). So

¹The source code for ReLU, Max Pooling and Shift-Accumulation operations on encrypted data is attached to the supplementary material.

Architectures	Required Depth (K)	Total Acc(%)
FCN C-B-A-P-C-P-F-B-A-F	1.4-0.3-3-2.4-1.4-2.4-3.1-0.3-4.6-2	21K 98.71
TCN C-B-A-P-C-P-F-B-A-F	1.4-0.3-0.1-0.2-0.2-0.2-3.1-0.3-0.1-2	9.0K 99.54
SHE C-B-A-P-C-P-F-B-A-F	0.2-0.3-0.1-0.2-0.2-0.4-0.3-0.1-0.3	2.0K 99.54
DSHE [C-B-A-C-B-A-P]x4-F-F [0.2-0.3-0.1-0.2-0.3-0.1-0.1]x4-0.7-0.5	6.8K 99.77	

Table 2. The required MD of prior LHECNNs. In the column of network architecture, C means a convolution layer; B is a batch normalization layer; A indicates a activation layer; P denotes a pooling layer; and F is a fully-connected layer. Acc represents the inference accuracy. The detailed DSHE architecture can be viewed in [8].

compared to TFHE, the homomorphic arithmetic shift in other HE schemes are much more expensive.

3.3. Mixed Bitwidth Accumulator

Besides homomorphic shifts, the logarithmically quantized CNN models require accumulations to perform inferences. The computational cost of a TFHE adder are proportional to its bitwidth. For instance, an 8-bit TFHE adder costs doubled computational cost compared to its 4-bit counterpart. We quantized the inputs, activations and weights into their 5-bit power-of-2 representations, since recent works [24, 25] show that a 5-bit AlexNet model degrades the inference accuracy by $< 0.6\%$. However, the accumulation intermediate results have to be represented by 16 bits. Otherwise, the inference accuracy may dramatically decrease. Accumulating 5-bit shifted results through 16-bit TFHE adders wastes substantial computational cost.

Therefore, we propose a mixed bitwidth accumulator shown in Figure 3(c) to avoid the unnecessary computational cost. A mixed bitwidth accumulator is a adder tree, where each node is an TFHE adder. And TFHE adders at different levels of the tree have distinctive bitwidths. At the bottom level ($layer_0$) of the tree, we use b -bit TFHE adders, where b is 5. Instead of 16-bits adders, $layer_1$ of the tree has $(b+1)$ -bit TFHE adders, since the sum of two 5-bit integers can have at most 6 bits. The n level of our mixed bitwidth accumulator consists of $(b+n)$ -bit TFHE adders.

3.4. Deeper Neural Network

The LHE mode of a HE scheme with a set of predefined parameters allows only a fixed *multiplicative depth* (MD), which is the maximal number of consecutively executed homomorphic AND gates in a LHE Boolean circuit [27]. We use DB to indicate the total MD budget of a LHE. The total MD required by an n -layer LHECNN is the sum of the MD (LD_i) of each layer, which is denoted by $\sum_{i=0}^n LD_i$. And LD_i can be defined as

$$LD_i = IN \cdot \log_2(KC^2) \cdot (DA[a] + DM[b]) + DR[c] + \log_2(KP^2) \cdot DM[d] \quad (1)$$

where IN is the input channel #; KC means the weight kernel size; $DA[a]$ is the MD required by an a -bit adder; $DM[b]$ indicates the MD required by a b -bit multiplier; $DR[c]$ is

the MD required by a c -bit *ReLU* unit; KP denotes the pooling kernel size; $DM[d]$ is the MD required by a d -bit max pooling unit. The LHECNN model must guarantee $DB \geq \sum_{i=0}^n LD_i$. Although it is possible to enlarge DB by re-designing another set of LHE parameters, the new set of LHE parameters increases the ciphertext size and prolongs the overall inference latency of the LHECNN. Considering the inference latency of prior LHECNNs is already hundreds of seconds, enlarging DB is not a promising way to achieve a deep network architecture. In fact, prior LHECNNs have huge MD in each layer, since they perform matrix multiplications and *square* activations, i.e., $DM[b]$ and $DR[c]$, are large. As Table 2 shows, in a FCN testing MNIST, each convolutional or fully-connected layer requires a $1K \sim 2K$ MD. In contrast, the activation or pool layer needs a $2 \sim 5K$ MD. As a result, they can support only shallow CNN models with less layers. The total MD of the MNIST FCN is $21K$. Moreover, FCN has to reduce the number of activation layers using larger weight kernel sizes and adding more fully-connected layers. These limitations of FCN result in only 98.71% accuracy on MNIST.

To obtain a deep network with more layers under a fixed DB , we need to reduce the MD (LD_i) required by each layer. After we created TCN by using our *ReLU* units, Max Pooling Units and the TFHE scheme to implement the network architecture of FCN testing MNIST, the total MD of TCN is reduced to $9.0K$ in Table 2, since the required MD by each activation or pool layer is greatly reduced by TFHE. When we further applied our power-of-2 quantization and mixed bitwidth accumulators, the total MD of SHE decreases to only 2032. This is because the TFHE shifter has 0 required MD while our mixed bitwidth accumulator also reduces its MD along its carry path. We further propose a deeper SHE (DSHE) architecture by adding more convolutional and activation layers. Compared to the 10-layer FCN, our 30-layer DSHE increases the MNIST inference accuracy to 99.77% with a required MD of 6.8K.

4. Experimental Methodology

TFHE setting and security analysis. Our schemes are implemented with the TFHE library [28]. We used all 3 levels of TFHE in the LHE mode. The level-0 TRLWE has the minimal noise standard variation $\underline{\alpha} = 6.10 \cdot 10^{-5}$, the count of coefficients $\underline{n} = 500$, and the security degree $\lambda = 194$ [19]. The level-1 TRLWE configures the minimal noise standard variation $\alpha = 3.29 \cdot 10^{-10}$, the count of coefficients $n = 1024$, and the security degree $\lambda = 152$. The level-3 TRGSW sets the minimal noise standard variation $\overline{\alpha} = 1.42 \cdot 10^{-10}$, the count of coefficients $\overline{n} = 2048$, the security degree $\overline{\lambda} = 289$. We adopted the same key-switching parameters as [19]. Therefore, SHE allows 32K depth of homomorphic AND primitive in the LHE mode [19]. The security degree of SHE is $\lambda = 152$.

Simulation, benchmark and dataset. We ran all experiments on an Intel Xeon E7-4850 CPU with 1TB DRAM. Our datasets include MNIST [6], CIFAR-10 [7], ImageNet [9] and the diabetic retinopathy dataset [4] (denoted by medicare). Medicare comprises retinal fundus images labeled by the condition severity including ‘none’, ‘mild’, ‘moderate’, ‘severe’, or ‘proliferative’. By following [4], we scaled the image of medicare to the same size of ImageNet, 224×224 . We also adopted the Penn Treebank dataset [29] to evaluate a LTFHE-enabled LSTM network.

Network architecture. The network architectures we estimated for various datasets are summarized in Table 3. For MNIST, we set SHE the same as CNT [2] and DSHE the same as [33]. For CIFAR-10, we adopted the architecture of SHE from [8] and that of DSHE from [30]. To evaluate Penn Treebank, we used the LSTM architecture from [29], where the activations of all LSTM gates are converted to *ReLU*. Compared to the original LSTM with various activation functions, e.g., *ReLU*, *sigmoid* and *tanh*, the LSTM with all *ReLU* has only $< 1\%$ accuracy degradation [29]. For ImageNet and Medical datasets, we adopted AlexNet [31], ResNet-18 [30] and ShuffleNet [32]. For all networks, we quantized weights into 5-bit power-of-2 representations, and converted inputs and activations to 5-bits fixed point numbers with little accuracy loss [24].

5. Results and Analysis

We report the inference latency and accuracy of encrypted neural networks through the numbers of homomorphic operations (HOPs), homomorphic gate operations (HGOPs) in Table 4~7. HOPs and HGOPs are independent of the hardware setting and software parallelization. Specifically, the HOP includes additions, multiplications, shifts and comparisons between ciphertext and plaintext. The multiplication between two ciphertexts (CC_{mult}) is the most computationally expensive operation among all HOPs, since it requires the largest number of homomorphic gate operations (HGOPs). We compared SHE against four the state-of-the-art LHECNN schemes including CNT [2], NED [3], FCN [4] and DiNN [1]. More details can be viewed in Table 1.

5.1. MNIST

As Table 4 shows, CNT obtains 98.95% accuracy by degree-2 polynomial approximation activations. The polynomial approximation errors prevent CNT from approaching the unencrypted state-of-the-art inference accuracy on MNIST. FCN slightly degrades the inference accuracy by 0.24% but shortens the inference latency by 84.3% by quantizing CNT and pruning its redundant weights. The weight pruning of FCN significantly decreases the numbers of CC_{Add} and PC_{Mult} . In contrast, FCN keeps the same number of activations, so it has the same number of CC_{Mult} occurring during only activations. DiNN uses the TFHE

cryptosystem and quantizes all network parameters (i.e., weights, inputs, and activations) to 1-bit, so it reduces the inference accuracy by 5.29%. Through increasing the degree of polynomial approximation activations, NED improves the inference accuracy by 0.58% over CNT. However, compared to CNT, it prolongs the inference latency by 28.2%, because it has much more CC_{Add} s, PC_{Mult} s and CC_{Mult} s to compute during an inference.

We used the TFHE cryptosystem to implement the network architecture of FCN (denoted by TCN) by using LTFHE-based *ReLU* activations, max poolings and matrix multiplications. Due to the *ReLU* activations and max poolings, TCN enhances the inference accuracy by 0.6% over FCN. But compared to FCN, it slows down the inference by 126.6%, since TFHE is not suitable to implement massive repetitive matrix multiplications. To create the SHE scheme, we further use power-of-2 quantized weights and replace matrix multiplications by LTFHE-based shift-accumulation operations in TCN. As a result, SHE maintains the same inference accuracy but greatly reduces the inference latency to 9.3s. We noticed that SHE requires only 2.0K multiplicative depth which is much smaller than our LTFHE noise budget, so we can use a deeper network architecture (DSHE) with more convolutional and activation layers. DSHE obtains 99.77% accuracy and spends 124.9s in an inference. We also reported the inference latency values of fully-TFHE-based TCN, SHE and DSHE. Compared to leveled-TFHE-based counterparts, they require much more time because of the computational expensive bootstrapping operations.

The size of encrypted message that a client sends to the cloud can be calculated by $Msize = PN \times SN \times PS$, where PN is the pixel number of the input image; SN means the polynomial number in a ciphertext; and PS indicates the size of a polynomial. PN is dependent on the dataset, while SN and PS are related to the cryptosystem parameters. For a MNIST image, $PN = 28 \times 28 = 784$. We quantized the inputs to 5-bit, so SHE encrypts each pixel in a MNIST image by 5 polynomials ($SN = 5$). In LTFHE, $PS = 32KB$. Totally, an MNIST image is encrypted into $784 \times 5 \times 32KB = 122.5MB$. Compared to other non-TFHE cryptosystems, SHE transfers much smaller message data between the client and the server. And typically, the encryption and decryption latency is proportional to the encrypted message size [4].

5.2. CIFAR-10

Only NED and FCN can support CIFAR-10, due to its large computational overhead. As Table 5 shows, compared to NED with high degree polynomial approximation activations, FCN reduces the inference accuracy by 16.2% but shortens the inference latency by 69.1%. With the same network architecture, TCN reduces the activation computational overhead of FCN, but it requires longer convolu-

Dataset	Network Architecture
MNIST	SHE: C-B-A-P-C-P-F-B-A-F [2]; DSHE: [C-B-A-C-B-A-P]X4-F-F [8]
CIFAR-10	SHE:[C-B-A-C-B-A-P] \times 3-F-F [8]; DSHE: ResNet-18 [30]
Penn Treebank	LSTM: time-step 25, 1 300-unit layer; <i>ReLU</i> ; [29]
ImageNet & Medical	AlexNet [31], ResNet-18 [30] and ShuffleNet [32]

Table 3. Network architecture (C means a convolution layer; A is a batch normalization layer and a activation layer; P indicates a pooling layer; and F is a fully-connected layer.).

Scheme	HOPs	CC_{Add}	PC_{Mult}	CC_{Mult}	PC_{Shift}	CC_{Com}	HGOPs	Depth	MSize	EDL(s)	FIL(s)	LIL(s)	Acc(%)
CNT	612K	312K	296K	945	0	0	-	134K	368MB	47.5	-	250	98.95
FCN	67K	38K	24K	945	0	0	-	21K	411MB	6.7	-	39.1	98.71
DiNN	16K	8K	8K	40	0	0	40K	80	66MB	0.0002	-	0.49	93.71
NED	4.7M	2.3M	2.3M	1.6K	0	0	-	172K	337MB	16.7	-	320	99.52
TCN	42K	19K	19K	0	0	3K	8.3M	8.8K	123MB	0.0014	108K \dagger	88.6	99.54
SHE	23K	19K	945	0	19K	3K	856K	2.0K	123MB	0.0014	11K \dagger	9.3	99.54
DSHE	613K	304K	5K	0	304K	5K	11.6M	6.2K	123MB	0.0014	149K \dagger	124.9	99.77

Table 4. The results on MNIST (HOPs: homomorphic operations; HGOPs: homomorphic gate operations; Depth: multiplicative depth; MSize: ciphertext message size; EDL: encryption and decryption latency; Acc: inference accuracy; FIL: fully TFHE inference latency; LIL: leveled TFHE inference latency; CC_{Add} : # of additions between two ciphertexts; PC_{Mult} : # of multiplications between a plaintext and a ciphertext; CC_{Mult} : # of multiplications between two ciphertexts; PC_{Shift} : # of shifts between a plaintext and a ciphertext; CC_{Com} : # of comparisons (including *ReLU* and max pooling) between two ciphertexts. \dagger denotes that we ran only its first 3 layers and made FIL values by projections.).

Scheme	HOPs	CC_{Add}	PC_{Mult}	CC_{Mult}	PC_{Shift}	CC_{Com}	HGOPs	Depth	MSize	EDL(s)	FIL(s)	LIL(s)	Acc(%)
NED	2.4G	1.2G	1.2G	212K	0	0	0	-	1.8GB	21.8	-	127K \dagger	91.50
FCN	610M	350M	350M	64K	0	0	0	69.8K	1.6GB	8.8	-	39K \dagger	76.72
TCN	8.7M	4.4M	4.4M	0	0	16K	2.8G	25.1K	160MB	0.0018	37M \dagger	31K \dagger	92.54
SHE	4.4M	4.4M	13K	0	4.4M	16K	211M	5.2K	160MB	0.0018	2.7M \dagger	2258	92.54
DSHE	68M	68M	98K	0	68M	131K	3.3G	13.7K	160MB	0.0018	42.5M \dagger	12041	94.62

Table 5. The results on CIFAR-10 (\dagger denotes that we ran only its first 3 layers and made FIL and LIL values by projections. Abbreviations are the same as Table 4).

tion latency. Overall, it reduces the inference latency by 20.5%. However, the *ReLU* activations and max poolings increase the inference accuracy to 92.54%. Compared to TCN, SHE reduces the number of PC_{Mult} by 99.7%. As a result, it improves the inference latency by 92.7% over TCN by performing only LTFHE shift-accumulation operations. Because SHE requires only 5.2K multiplicative depth which is much smaller than our LTFHE noise budget 32K, we use a deeper network, DSHE, to increase the inference accuracy to 96.62% and the inference latency to 12041s.

5.3. ImageNet and Medical Datasets

No prior LHECNN model supports the entire inference on an ImageNet picture, because of its prohibitive computational overhead. FCN [4] can compute inferences for the last 3 layers of a network testing ImageNet. In Table 6, SHE uses the network architectures of AlexNet, ResNet-18 and ShuffleNet for inferences on ImageNet. For AlexNet and ResNet-18, TCNs ask for $>32K$ multiplicative depth which is larger than our LTFHE noise budget. Therefore, TCN cannot work on them. On the contrary, SHE needs 1 day and 2.5 days to test an ImageNet picture by AlexNet and ResNet-18, respectively. Particularly, SHE requires only 5 hours to test an ImageNet image and achieves 69.4% top-1 accuracy by the ShuffleNet topology. For the medical dataset, it ob-

tains 71.32% inference accuracy. Besides shorter latency and higher accuracy, SHE enables a much deeper architecture under a fixed LTFHE noise budget, since the LTFHE shifts increase little multiplicative depth. SHE is the critical enabler to construct accurate and deep LHECNN models, e.g., AlexNet, ResNet-18 and Shufflenet.

5.4. Penn Treebank

No prior LHECNN model supports LSTM, since it asks for huge multiplicative depth. As Figure 4(a) shows, the required multiplicative depth of the matrix multiplication in all time steps between H_{t-1} and X_t is 4.7K (caculated by Equation 1) \times 25 = 117.5K which is already larger than current 32K LTFHE noise budget. Therefore, TCN cannot successfully implement the LSTM architecture. We use SHE to build a LSTM network to predict the next word on Penn Treebank as Figure 4(b) shows where SHE using shifts and accumulations with small multiplicative depth to replace expensive matrix multiplications, only costs 0.5K multiplicative depth in the multiplications between between H_{t-1} and X_t . SHE costs total 30K depth which is below the threshold of 32K LTFHE noise budget like the Table 7 shows. The accuracy of LSTM on Penn Treebank is measured by Perplexity Per Word (PPW). SHE obtains 89.8 PPW. Compared to the full-precision LSTM on plaintext data, it degrades the

Network Scheme	HOPs	CC_{Add}	PC_{Mult}	PC_{Shift}	CC_{Com}	HGOPs	Depth	MSize	EDL(s)	FIL(s)	LIL(s)	$Acc_I(\%)$	$Acc_M(\%)$	
AlexNet	TCN	0.3G	0.14G	0.14G	0	0.66M	38G	42.3K	7.7GB	0.07	-	-	-	
	SHE	0.14G	0.14G	0.4M	0.14G	0.34M	5.5G	6.8K	7.7GB	0.07	72M†	89K†	54.17	63.24
ResNet	TCN	0.7G	0.36G	0.36G	0	2.47M	100G	96.4K	7.7GB	0.07	-	-	-	-
	SHE	0.36G	0.36G	1.1M	0.36G	0.49M	15G	13.7K	7.7GB	0.07	195M†	0.23M†	66.8	67.29
Shuffle	TCN	56M	0.14G	0.14G	0	1.37M	7.9G	27.1K	7.7GB	0.07	102M†	126K†	69.4	71.32
	SHE	28M	28M	83K	28M	275K	1.1G	3.9K	7.7GB	0.07	14M†	18K	69.4	71.32

Table 6. The results on ImageNet and Medical dataset (Acc_I means the inference accuracy of ImageNet, while Acc_M denotes the inference accuracy of the medical dataset. The other abbreviations are the same as Table 4. † denotes that we ran only its first 3 layers and made FIL and LIL values by projections.).

Scheme	HOPs	CC_{Add}	PC_{Mult}	PC_{Shift}	CC_{Com}	HGOPs	Depth	MSize	EDL(s)	FIL(s)	LIL(s)	PPW
TCN	576K	270K	270K	0	36K	75.7M	143K	9.4MB	0.014	-	-	-
SHE	336K	270K	30.4K	243K	36K	24.4M	30K	9.4MB	0.014	318K†	576	89.8

Table 7. The results on Penn Treebank (Abbreviations are the same as Table 4. † denotes that we ran only its first 3 layers and made FIL values by projections.).

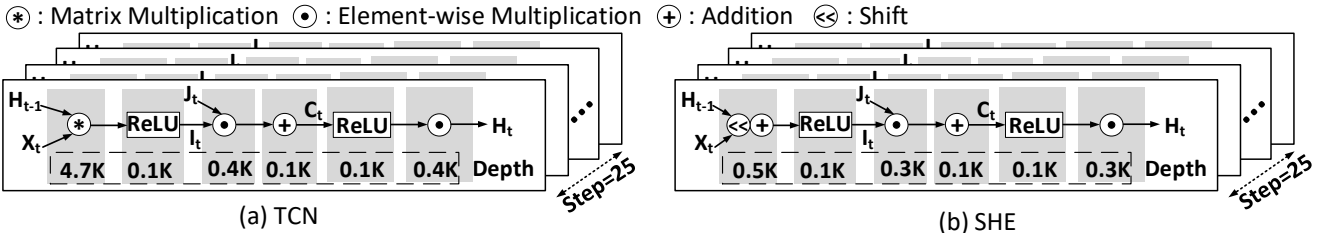


Figure 4. Required multiplicative depth breakdown of FCN and SHE implementations on ReLU-based LSTM where we use TFHE-friendly ReLU to replace sigmoid and tanh activations inspired by [29]. 25 timesteps of LSTM share the same function and computational process which takes previous layer’s output H_{t-1} and current input word X_t in Penn Treebank as inputs and generates output H_t .

inference accuracy by only 2.1%. It takes 576s for SHE to conduct an inference on the dataset of Penn Treebank.

6. Conclusion

In this paper, we propose SHE to overcome the polynomial approximation activations and poolings by using TFHE and logarithmic quantization. We present a *ReLU* unit, a max pooling unit and a mixed bitwidth accumulator to accelerate SHE inference and reduce its required multiplicative depth. Our experimental results show SHE achieves the state-of-the-art inference accuracy and reduces the inference latency by 76.21% ~ 94.23% over prior LHECNNs on various datasets. SHE is the first LHE-enabled model that can support deep CNN architectures on ImageNet and LSTM architectures on Penn Treebank.

References

- [1] Florian Bourse, Michele Minelli, Matthias Minihold, and Pascal Paillier. Fast homomorphic evaluation of deep discretized neural networks. In Hovav Shacham and Alexandra Boldyreva, editors, *Advances in Cryptology – CRYPTO 2018*, pages 483–512. Springer International Publishing, 2018.
- [2] Nathan Dowlin, Ran Gilad-Bachrach, Kim Laine, Kristin Lauter, Michael Naehrig, and John Wernsing.
- [3] Ehsan Hesamifard, Hassan Takabi, and Mehdi Ghasemi. Deep neural networks classification over encrypted data. In *ACM Conference on Data and Application Security and Privacy*, pages 97–108. ACM, 2019.
- [4] Edward Chou, Josh Beal, Daniel Levy, Serena Yeung, Albert Haque, and Li Fei-Fei. Faster cryptonets: Leveraging sparsity for real-world encrypted inference. *CoRR*, abs/1811.09953, 2018.
- [5] Amartya Sanyal, Matt J. Kusner, Adrià Gascón, and Varun Kanade. TAPAS: tricks to accelerate (encrypted) prediction as a service. *CoRR*, abs/1806.03461, 2018.
- [6] Yann LeCun and Corinna Cortes. MNIST handwritten digit database. Technical report, New York University, 1998.
- [7] Alex Krizhevsky. Learning multiple layers of features from tiny images. Technical report, University of Toronto, 2009.

[8] Hervé Chabanne, Amaury de Wargny, Jonathan Milgram, Constance Morel, and Emmanuel Prouff. Privacy-preserving classification on deep neural network. *IACR Cryptology ePrint Archive*, 2017:35, 2017.

[9] J. Deng, W. Dong, R. Socher, L.-J. Li, K. Li, and L. Fei-Fei. ImageNet: A Large-Scale Hierarchical Image Database. In *2009 Conference on Computer Vision and Pattern Recognition*, 2009.

[10] Craig Gentry et al. Fully homomorphic encryption using ideal lattices. In *ACM Symposium on Theory of Computing*, volume 9, pages 169–178, 2009.

[11] Craig Gentry, Amit Sahai, and Brent Waters. Homomorphic encryption from learning with errors: Conceptually-simpler, asymptotically-faster, attribute-based. In Ran Canetti and Juan A. Garay, editors, *Advances in Cryptology – CRYPTO 2013*, pages 75–92, Berlin, Heidelberg, 2013. Springer Berlin Heidelberg.

[12] Zvika Brakerski, Craig Gentry, and Vinod Vaikuntanathan. (leveled) fully homomorphic encryption without bootstrapping. *ACM Transactions on Computation Theory (TOCT)*, 6(3):13, 2014.

[13] P. Mohassel and Y. Zhang. Secureml: A system for scalable privacy-preserving machine learning. In *IEEE Symposium on Security and Privacy*, pages 19–38, May 2017.

[14] Jian Liu, Mika Juuti, Yao Lu, and N. Asokan. Oblivious neural network predictions via minionn transformations. *Cryptology ePrint Archive*, Report 2017/452, 2017. <https://eprint.iacr.org/2017/452>.

[15] Bita Darvish Rouhani, M. Sadegh Riazi, and Farinaz Koushanfar. Deepsecure: Scalable provably-secure deep learning. In *Design Automation Conference*, pages 2:1–2:6, New York, NY, USA, 2018. ACM.

[16] Christina Boura, Nicolas Gama, and Mariya Georgieva. Chimera: a unified framework for b/fv, tfhe and heaan fully homomorphic encryption and predictions for deep learning. *Cryptology ePrint Archive*, Report 2018/758, 2018. <https://eprint.iacr.org/2018/758>.

[17] Nishanth Chandran, Divya Gupta, Aseem Rastogi, Rahul Sharma, and Shardul Tripathi. Ezpc: Programmable, efficient, and scalable secure two-party computation for machine learning. In *(IEEE EuroS&P 2019)*, February 2019.

[18] Chiraag Juvekar, Vinod Vaikuntanathan, and Anantha Chandrakasan. GAZELLE: A low latency framework for secure neural network inference. In *USENIX Security Symposium*, pages 1651–1669, Baltimore, MD, 2018. USENIX Association.

[19] Ilaria Chillotti, Nicolas Gama, Mariya Georgieva, and Malika Izabachène. Tfhe: Fast fully homomorphic encryption over the torus. *IACR Cryptology ePrint Archive*, 2018:421, 2018.

[20] Ahmad Qaisar Ahmad Al Badawi, Yuriy Polyakov, Khin Mi Mi Aung, Bharadwaj Veeravalli, and Kurt Rohloff. Implementation and performance evaluation of rms variants of the bfv homomorphic encryption scheme. *IEEE Transactions on Emerging Topics in Computing*, 2019.

[21] Shai Halevi, Yuriy Polyakov, and Victor Shoup. An improved rns variant of the bfv homomorphic encryption scheme. In *Cryptographers’ Track at the RSA Conference*, pages 83–105. Springer, 2019.

[22] Jung Hee Cheon, Andrey Kim, Miran Kim, and Yongsoo Song. Homomorphic encryption for arithmetic of approximate numbers. In *International Conference on the Theory and Application of Cryptology and Information Security*, pages 409–437. Springer, 2017.

[23] Alon Brutzkus, Oren Elisha, and Ran Gilad-Bachrach. Low latency privacy preserving inference. *CoRR*, abs/1812.10659, 2018.

[24] Aojun Zhou, Anbang Yao, Yiwen Guo, Lin Xu, and Yurong Chen. Incremental network quantization: Towards lossless cnns with low-precision weights. *CoRR*, abs/1702.03044, 2017.

[25] Denis A Gudovskiy and Luca Rigazio. Shiftcnn: Generalized low-precision architecture for inference of convolutional neural networks. *arXiv preprint arXiv:1706.02393*, 2017.

[26] Song Han, Huizi Mao, and William J Dally. Deep compression: Compressing deep neural networks with pruning, trained quantization and huffman coding. *arXiv preprint arXiv:1510.00149*, 2015.

[27] M. Sadegh Riazi, Christian Weinert, Oleksandr Tkachenko, Ebrahim M. Songhor, Thomas Schneider, and Farinaz Koushanfar. Chameleon: A hybrid secure computation framework for machine learning applications. In *Proceedings of the 2018 on Asia Conference on Computer and Communications Security*, pages 707–721, New York, NY, USA, 2018. ACM.

[28] Ilaria Chillotti, Nicolas Gama, Mariya Georgieva, and Malika Izabachène. TFHE: Fast fully homomorphic encryption library, August 2016. <https://tfhe.github.io/tfhe/>.

- [29] Quoc V. Le, Navdeep Jaitly, and Geoffrey E. Hinton. A simple way to initialize recurrent networks of rectified linear units. *CoRR*, abs/1504.00941, 2015.
- [30] Kaiming He, Xiangyu Zhang, Shaoqing Ren, and Jian Sun. Deep residual learning for image recognition. *CoRR*, abs/1512.03385, 2015.
- [31] Alex Krizhevsky, Sutskever Ilya, and Geoffrey Hinton. Imagenet classification with deep convolutional neural networks. In *Advances in neural information processing systems*, 2012.
- [32] Xiangyu Zhang, Xinyu Zhou, Mengxiao Lin, and Jian Sun. Shufflenet: An extremely efficient convolutional neural network for mobile devices, 2017.
- [33] Dan C. Ciresan, Ueli Meier, and Jürgen Schmidhuber. Multi-column deep neural networks for image classification. *CoRR*, abs/1202.2745, 2012.